Optimal Subassembly Partitioning of Space Frame Structures for In-Process Dimensional Adjustability and Stiffness

Naesung Lyu
Department of Mechanical Engineering,
University of Michigan,
Ann Arbor, MI 48109-2125
e-mail: nlyu@umich.edu

Byungwoo Lee
General Electric Global Research Center,
Niskayuna, NY 12309
e-mail: leeb@research.ge.com

Kazuhiro Saitou[1]
Department of Mechanical Engineering,
University of Michigan,
Ann Arbor, MI 48109-2125
e-mail: kazu@umich.edu

A method for optimally synthesizing multicomponent structural assemblies of an aluminum space frame (ASF) vehicle body is presented, which simultaneously considers structural stiffness, manufacturing and assembly costs and dimensional integrity under a unified framework based on joint libraries. The optimization problem is posed as a simultaneous determination of the location and feasible types of joints in a structure selected from the predefined joint libraries, combined with the size optimization for the cross sections of the joined structural frames. The structural stiffness is evaluated by finite element analyses of a beam-spring model modeling the joints and joined frames. Manufacturing and assembly costs are estimated based on the geometries of the components and joints. Dissimilar to the enumerative approach in our previous work, dimensional integrity of a candidate assembly is evaluated as the adjustability of the given critical dimensions, using an internal optimization routine that finds the optimal subassembly partitioning of an assembly for in-process adjustability. The optimization problem is solved by a multiobjective genetic algorithm. An example on an ASF of the midsize passenger vehicle is presented, where the representative designs in the Pareto set are examined with respect to the three design objectives. [DOI: 10.1115/1.2181599]

1 Introduction

Many modern mechanical products, such as ships hulls, airplanes, and automotive bodies, are so complex that it is almost impossible (or too expensive) to be manufactured in one piece. Therefore, most products are made of many components joined together. Hence, during the conceptual stage of such products, designers need to determine the set of components and the methods of joining the components by decomposing the entire product geometry. In the automotive industry, for example, a handful of basic decomposition schemes considering geometry, functionality, and manufacturing issues have been applied in this process. However, these decomposition schemes depend mainly on the designers' experiences, which may cause the following problems:

1. Insufficient stiffness of assembled structure: Structural characteristics of two components joined together are generally different from the one of a component of the same geometry without a joint, and the difference largely depends on the location and geometry of joints and joining methods. Therefore, improper decisions on these may cause assembled structures to be incapable of satisfying the desired stiffness specifications.
2. Manufacturing and/or assembly problems: Feasibility and difficulty in manufacturing and assembly of components largely depend on the geometry of components and joints, and assembly processes. Therefore, unsystematic decisions on these may lead to a design that cannot be economically manufactured and/or assembled.
3. Insufficient adjustability for critical dimensions: To reduce the cost of producing high-tolerance components, the dimensional integrity in large-scale assemblies is often achieved by the adjustment of the critical product dimensions (key characteristics, KC [1]) during assembly processes when the parts are located in fixtures. To enable these *in-process dimensional adjustments*, joints must allow a small relative motion along the direction of the KC at the assembly step where the KC is being achieved (Fig. 1). Therefore, unsystematic decisions on the location and geometry of joints and assembly sequences may prevent the in-process adjustability of critical dimensions, leading to the poor dimensional integrity of assembled structures.

The above three problems are usually found in the production/testing phases and require expensive and time-consuming iteration procedures. Therefore, introducing a cost effective but systematic optimization method in determining the components set considering overall structural characteristics, manufacturing and assembly costs, and dimensional integrity altogether will have a significant impact on industry.

Assembly synthesis is a process of determining the optimal components set through the decomposition of the end product design prior to the detailed component design phase [3]. As an extension of our past works on the decomposition-based assembly synthesis [3–9], this paper introduces a method for determining the components set of aluminum space frame (ASF) vehicle bodies using preanalyzed joint libraries defined at each potential joint location. The uniqueness of the present work is the integration of the criteria on stiffness, manufacturing and assembly costs [5,8], and the criteria on dimensional adjustablility [6,7] to a multicriteria optimization problem under a unified framework based on joint libraries. In our previous work [6,7], dimensional adjustability was regarded as the only criterion an assembly should meet, and a binary decomposition algorithm was developed that enumerates all component designs and joint configurations satisfying

[1]Corresponding author.

Contributed by the Design Automation Committee of ASME for publication in the JOURNAL OF MECHANICAL DESIGN. Manuscript received August 4, 2004; final manuscript received August 11, 2005. Review conducted by Wei Chen.

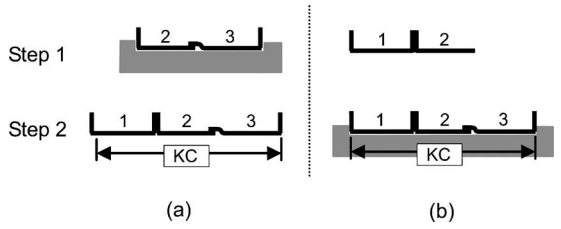

Fig. 1 Two assembly sequences for automobile floor pan design (modified from [2]), where the total length is the critical dimension (KC). (*a*) Poor design (cannot adjust total length in the final assembly) and (*b*) better design (can adjust total length in the final assembly).

the adjustability of given critical dimensions. The algorithm takes full advantage of the fact that dimensional adjustability is a separable criterion; namely, the dimensional adjustability of an entire assembly can be broken down to a set of criteria for subassemblies, each of which must be met at every assembly step. While highly effective when dimensional adjustability is the only criterion, this approach does not allow a straightforward integration with fundamentally global criteria, such as structural stiffness, which does not allow clear separation into equivalent criteria for subassemblies. To overcome this problem, this paper adopts a novel subassembly partitioning method for dimensional adjustability evaluation [4], which allows an elegant integration of the stiffness, manufacturing and assembly costs, and dimensional adjustability criteria within a framework of multiobjective optimization.

The paper is organized as follows: Related works are presented in the next section. Then the methods for synthesizing multicomponents ASF using the joint library are proposed and mathematically formulated as a optimization problem. A case study on an aluminum space frame (ASF) of a passenger vehicle is presented and results are discussed.

2 Related Work

2.1 DFA/DFM and Assembly Synthesis. Boothroyd and Dewhurst [9] are regarded as major establishers of design for assembly (DFA) and design for manufacturing (DFM) concepts, a collection of design methods to identify and alleviate manufacturing problems at the product design stage. They proposed to minimize the total assembly cost with the reduction of part count, followed by the local design changes of the remaining parts. Conventional DFA/DFM methods assume the predetermined components with given geometries and, therefore, are limited to the design improvements by locally modifying the given geometries. Decomposition-based assembly synthesis [3–7], on the other hand, emphasizes the determination of components prior to the detailed design stages. Starting with no prescribed components, the method decomposes the component geometry so the optimal components set and joint configurations best achieving the design criteria on each component and joint, as well as the assembles product. The criteria attempted in the previous work includes structural strength [3], structural stiffness [5,6], and dimensional integrity [4,7].

2.2 Automotive Body Structure Modeling. During the early stage of automotive body-in-white (BIW) design procedures, simple beam/spring models are widely used. In the beam/spring models, difficulties often arise in modeling the structural property of joints. Modeling joints as torsional springs is a popular method [10] due to its simplicity, and the equivalent torsional spring rates of the joints are identified from physical or numerical (by using detailed finite element analysis (FEA) models) experiments. Lee and Nikolaidis [11] proposed a 2D joint model considering the flexibility of joints, the offset of rotation centers, and coupling effects between the movements of joint branches. Kim and Kim discussed the accuracy of FEA based joint rate evaluations regarding transformation error from a shell element model to spring rate and proposed their own model [12]. Long [13] presented two tools that link the performance targets for a joint in a BIW to its geometry. The first tool, called translator A, predicts the structural performance of a given joint geometry using artificial neural network (ANN) and response surface method (RSM). The second tool, called translator B, solves the inverse problem of finding a joint geometry that meets the given performance targets, using the translator A and sequential quadratic programming (SQP). The above works, however, mainly focused on the analyses of structural properties of joints, separately or as an integral of an overall structure and do not addresses the automated synthesis of joint locations and designs within a BIW as addressed in this paper.

2.3 Aluminum Space Frame (ASF) Design. Aluminum applications in the automotive industries have drawn a significant attention in the last two decades mainly due to the increasing demands on the high gas-mileage, light-weight, and environment-friendly vehicles. Since the BIW accounts for about one third of the total weight of a passenger vehicle, a significant amount of researches have been concentrated on this area [14,15], resulting in a number of mass-produced vehicles with ASF including Audi's A2 and A8, etc. [16].

Ahmetoglu [17] discussed the design of extruded profiles, bending, friction and formability of aluminum components for ASF body design. Chung et al. [18] studied the joint designs of an ASF by comparing FE models with experimental results. Motivated by the increased attention to ASF vehicle bodies, this paper provides a method of determining the optimal component set and joint configurations of ASF vehicle bodies considering structural characteristics, manufacturing cost, assembly cost, and dimensional adjustability.

2.4 Dimensional Integrity. The key characteristics (KC) are defined by Lee and Thornton [1] as product features, manufacturing process parameters, and assembly features that significantly effect a product's performance, function, and form. As it can be a challenging task to satisfy KC in the complex assembly with multiple components, our previous work [6,7] discussed an algorithm of assembly synthesis focused on the in-process adjustability and nonforced fit. The algorithm enumerates *all* possible assembly syntheses with the accompanying assembly sequences which, in combination, achieve dimensional adjustability for critical dimensions (key characteristics) and nonforced fit between parts. Noting that the dimensional adjustability of an entire assembly is separable to a set of equivalent criteria for subassemblies, the algorithm recursively decomposes a product from its final shape into parts and assigns joint configurations according to simple rules drawn from a related literature on assembly design [2]. Based on the AND/OR graph for assembly sequence planning [19], an augmented AND/OR graph has been devised to represent the results. As mentioned earlier, however, this approach does not allow a straightforward integration with intrinsically global criteria such as structural stiffness, which are generally inseparable to equivalent criteria for subassemblies. As an alternative to the enumeration-based approach, a subassembly partitioning method for optimal in-process dimensional adjustability has been developed [4]. In the method, each candidate assembly generated by a genetic algorithm is evaluated using an internal optimization routine that finds optimal subassembly partitioning for in-process adjustability sequentially (greedy approach), by solving an equivalent minimum cut problem on weighted graphs at each partitioning step.

While the usual design procedures consider the structural characteristics of the ASF structure and the dimensional adjustability as the separate problem and treat these two problems sequentially, this paper introduces the method that can treat both problems in one single optimization problem. Since the enumeration method

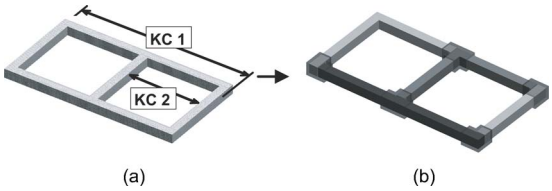

Fig. 2 (*a*) A sample space frame structure with two KCs (KC1, KC2), and (*b*) a possible components set with 4 components, shown in different shades

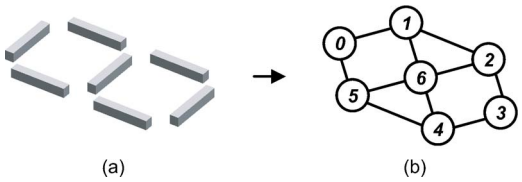

Fig. 4 (*a*) Seven basic members and (*b*) structural topology graph with seven nodes and ten edges

in [6,7] exhibits difficulty in the integration of a global criteria such as structural stiffness, the approach in [4] is adopted in the present paper due to its compatibility to the evaluation of structural stiffness and the manufacturing and assembly costs [6,8].

3 Approach

This section describes the methods for synthesizing multicomponents ASF using the joint library which simultaneously identify the optimal components set and component/joint designs considering the stiffness of the assembled structure, manufacturing/assembly cost, and dimensional adjustability. These methods consist of the following two major steps:

1. Geometry of the entire structure is transformed into a *structural topology graph*, representing the liaisons between *basic members*, the smallest decomposable components of the given structure, identified by the potential joint locations specified by the designer.
2. The product topology graph is decomposed through an optimization procedure into the subgraphs representing components by using a set of joints in the joint library.

Details of the above two steps are described below, with a sample space frame structure shown in Fig. 2. As illustrated in Fig. 2(*b*), it is assumed that frames are extruded tubes, bent or welded with cast "sleeves" at joints, following a typical construction of ASF structures.

3.1 Step 1: Construction of Structural Topology Graph. The method requires the designer to specify the potential joint locations to guarantee the feasibility of the final design to frame manufacturing and joining methods.

Figure 3 illustrates an example of six potential joint locations shown as grey boxes. For each potential joint location, the designer specifies feasible (potentially different) joint types to be included in the joint library. For example, four joint types (a1–a4) are assumed as available at location A in Fig. 3. Each joint type is associated with the joint design variables specifying the cross sections of the joined frames and the amount of welds, with which the structural properties of a joint are determined as described in the next section.

The basic members can be identified from the specified potential joint locations (Fig. 4(*a*)) and the structural topology graph $G=(M,T)$ is constructed from the basic members (Fig. 4(*b*)) such that

- Basic member m_i is represented as a node n_i in M.
- The liaison between two basic members m_i and m_j is represented as edge $e=\{n_i,n_j\}$ in T.

3.2 Step 2: Decomposition of Structural Topology Graph. The structural topology graph $G=(M,T)$ is decomposed by selecting a joint type in the library at each potential joint location. Based on the selected joint types, the corresponding edges in G are removed and G is decomposed into subgraphs. For example, by selecting joint type a3 in the joint library for location A in Fig. 5, the corresponding edges $\{1,2\}$ and $\{1,6\}$ are removed.

The selection of joint types and the removal of the corresponding edges in G result in subgraphs of G, each of which corresponds to a component. The cross-sectional dimensions of a component are then set as the averages of the ones in the joining frames (basic members) associated with the selected joint types in the component, which are subsequently used for retrieving the precomputed structural properties of the joints from the joint library. The selection of the joint types in Fig. 5, for example, results in four subgraphs (Fig. 6(*a*)) and the corresponding components (Fig. 7(*b*)).

Within an optimization loop, a decomposed structure consisting

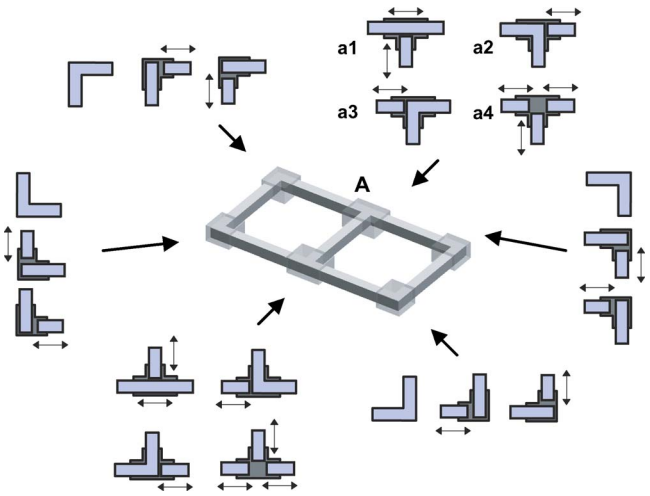

Fig. 3 Potential joint locations (grey boxes) and possible joint types at each location (joint library). Arrow(s) near each joint type indicates the adjustable direction during assembly.

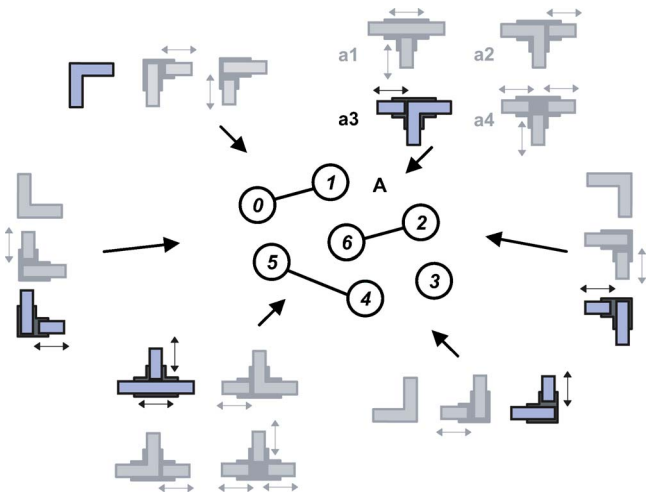

Fig. 5 Selected joint types and topology graph with the corresponding edges removed

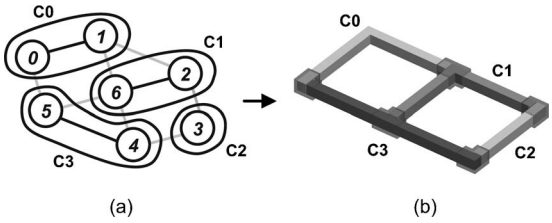

Fig. 6 (*a*) four subgraphs and (*b*) corresponding four components

of components and joints obtained as above is evaluated based on structural stiffness, manufacturing/assembly costs, and dimensional adjustability. While this paper addresses stiffness as a structural criterion, other structural criteria, such as crash worthiness, can be incorporated by using appropriate structural analyses.

1. Structural Stiffness: As in [6], the structural stiffness of the assembled structure is evaluated as a negative of the displacements at the specified locations in the assembled structure under given loading conditions. The displacements are calculated using the finite element analyses, where the components and all the joints are modeled as beam elements and torsion spring elements, respectively. As an example, a structure with four components in Fig. 7 (left) is modeled as a beam-spring FE model in Fig. 7 (right), where, the T joint is modeled as three beam elements connected by torsional spring elements k_0, k_1, and k_2. Each of the three spring elements has torsional stiffness (rate) around each of the three local orthogonal axes attached to the joint. Similar to this T joint, all the other joint locations are modeled using three torsional spring elements. The rate of the torsional spring elements are estimated by the finite element analyses of the detailed model of the joint. The values of the torsional spring rates for typical joint types, cross-sectional dimensions of the joined frames, and amount of welds are precomputed to produce a set of training data for an artificial neural network (ANN) that implements the joint library. Fully trained ANN gives the approximated spring rates from given physical joint design without running additional FE analysis for the joint. Therefore, similar to the translator A of [12], the trained ANN allows the spring rates of a joint to simply be retrieved from the joint library without the computational overheads due to the detailed FE analysis to get the joint spring rates.
2. Manufacturing/Assembly Cost: The manufacturing cost of components is evaluated as a negative of the total cost of producing components. As stated earlier, it is assumed that frames are extruded tubes, bent or welded with cast "sleeves" at joints, following a typical construction method of ASF. The cost of producing components is estimated by the sum of the cost of extrusion die (assumed as proportional to the size and complexity of the frame cross sections) and the cost of bending operations (assumed as proportional to the number of bending). The cost of producing cast sleeves is estimated by the cost of casting, which is assumed as simply proportional to its volume. The assembly cost is calculated as a negative of the total cost of joining. The method of joining is assumed to be the GMAW (gas metal arc welding), widely used for ASF. The welds are applied between the frames and the cast sleeves at joints. The cost is assumed to be proportional to the volume of total welds, calculated from the total welding length multiplied by weld thickness. Total manufacturing/assembly cost is the sum of manufacturing and assembly costs.
3. Dimensional adjustability: Dimensional adjustability of candidate component set and joint types is evaluated by estimating the in-process adjustability of the KCs. Adopting the approach in [4], this is done by an internal routine that computes a subassembly partitioning of given component set and joint type for optimal in-process adjustability, by solving the equivalent minimum cut problem on the weighted graphs.

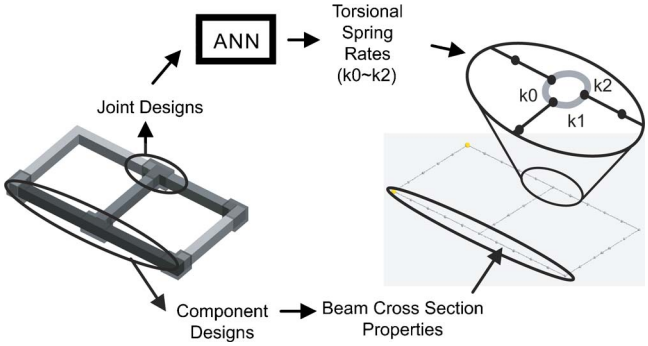

Fig. 7 A sample structure with four components and its beam-spring FE model

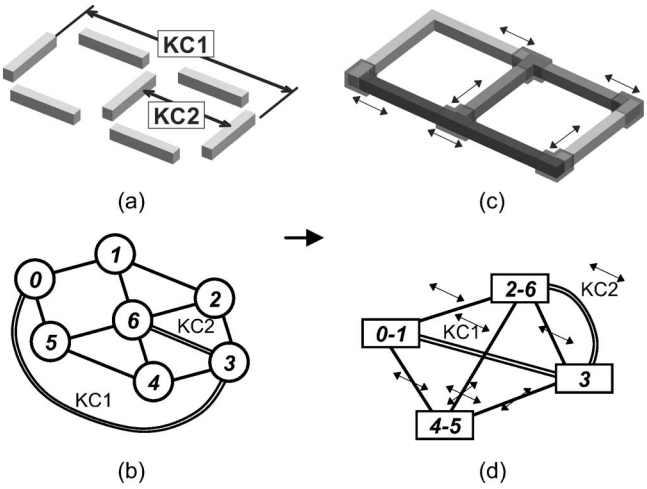

Fig. 8 (*a*) Basic members and (*b*) corresponding configuration graph $C=(M,T,A)$. (*c*) A sample components set design and (*d*) corresponding liaison graph L_0.

First, the structural topology graph $G=(M,T)$ is transformed to a configuration graph, $C=(M,T,A)$, where A is the set of edges representing the KCs between a pair of basic members (double-line edges in Fig. 8(*b*)). Note that two KCs in the structure (Fig. 8(*a*)) are represented as two edges $\{0,3\}$ and $\{3,6\}$ in C. With a joint type at each potential location, the configuration graph is transformed to a liaison graph $L_0=(V_0,E_0,A_0)$, where V_0 is the set of nodes representing parts, E_0 is the set of edges representing joints, and A_0 is the set of edges representing KCs. The A_0 takes over all the KCs from the A, but connecting the nodes in V_0 that are hypernodes of the nodes in M (since a part can consist of one or morenodes). The assembly represented as L_0 is evaluated for dimensional adjustability by the internal routine for subassembly partitioning (Fig. 9), until all KCs are broken, to check if adjustability is guaranteed for all KCs. Then the reverse of this subassembly partitioning yields a partial assembly sequence providing adjustability for all KCs [4].

Two-step partitioning of the given assembly is illustrated in Fig. 9, where the first partitioning (Fig. 9(*b*)) cut two edges $\{0-1,2-6\}$ and $\{0-1,4-5\}$ in L_0 to satisfy the KC1, resulting two subassemblies in Fig. 9(*c*). The second partitioning (Fig. 9(*d*)) is done by cutting two edges $\{2-6,3\}$ and $\{2-6,4-5\}$ to satisfy KC2.

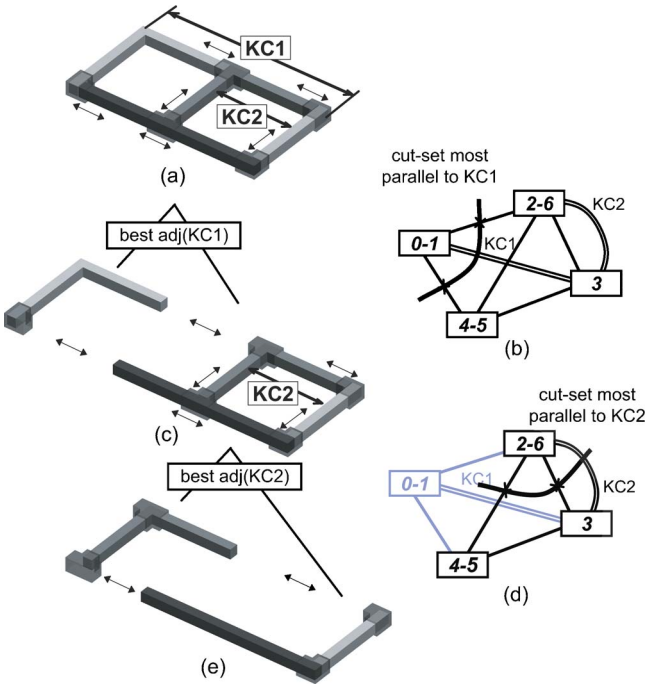

Fig. 9 Partitioning with best adjustability

Each partitioning is done by finding the optimal cut set of edges whose adjustable directions are most parallel to the KC. Figure 10 illustrates details of the first partitioning in Fig. 9. To find the optimal cut set, directional unit vectors are assigned to the edges in the liaison graph ($\mathbf{k}(a)$ for KC and $\mathbf{n}(e)$ for each edge e in Fig. 10(a))). Then the weight of each edge is defined and assigned as

$$1 - |\mathbf{k}(a) \cdot \mathbf{n}(e)| \tag{1}$$

The weight calculated from Eq. (1) will yield 0 when the joint has the perfect adjustability (parallel to KC) while the joint with imperfect adjustability (nonparallel to KC) will have nonzero weight measuring their counter adjustability. The optimal cut set to satisfy the given KCs will be obtained by finding the cut set of edges whose weights minimize the following equation:

$$\sum_{a \in \mathrm{KC}_p} \sum_{e \in \mathrm{CS}_p} (1 - |\mathbf{k}(a) \cdot \mathbf{n}(e)|) \tag{2}$$

where a is the KC in the KC_p, the set of KCs broken by the pth partitioning, and e is a joint in CS_p, the cut-set edges by the pth partitioning. In the example of Fig. 14, KC_p={KC1}. The optimal CS_p is $\{\{0-1,2-6\},\{0-1,4-5\}\}$ resulting the minimum value of Eq. (2) as 0.0 (perfect adjustability: all joints in $\{0-1,2-6\}$ and $\{0-1,4-5\}$ are parallel to the KC1).

Figure 11 illustrates a binary tree representation of the subassembly partitioning in Fig. 10. The entire adjustability is evaluated as the summation of the values calculated using Eq. (2) for entire partitioning. Further details can be found in [4].

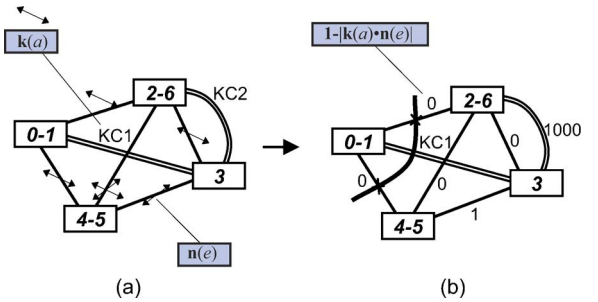

Fig. 10 Detailed procedures for finding the optimal cut in the first partitioning of Fig. 9(*b*)

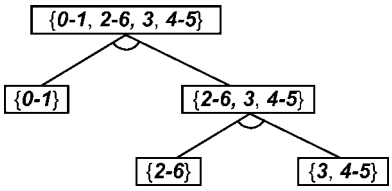

Fig. 11 Binary tree representation of the subassembly partitioning illustrated in Fig. 10

3.3 Mathematical Formulation

3.3.1 Definition of Design Variables. A design is uniquely specified by (1) the joint types at all possible joint locations, (2) the cross-sectional dimensions of all basic members, and (3) the amount of welds at all joints, which are represented by three vectors $\boldsymbol{x}$, $\boldsymbol{y}$, and $\boldsymbol{z}$, respectively:

$$\boldsymbol{x} \in J_1 \times J_2 \times \cdots \times J_n$$

$$\boldsymbol{y} \in S^B$$

$$\boldsymbol{z} \in W^n \tag{3}$$

where n is the number of possible joint locations in the structure, B is the number of basic members in the structure, J_i is the joint library at the i-th possible joint locations, S is the set of feasible cross-sectional dimensions, and W is the set of feasible amount of welds.

Note the elements of vectors $\mathbf{y}$ and $\mathbf{z}$ can also be vectors depending on the definitions of S and W, which appear in the following case study.

3.3.2 Definition of Objective Functions. Using the design variables $\boldsymbol{x}$, $\boldsymbol{y}$, and $\boldsymbol{z}$, the three objective functions described in the previous section are given as follows:

$$f_{\mathrm{stiff}}(\boldsymbol{x},\boldsymbol{y},z) = -\,\mathrm{DISP}(\mathrm{XSEC}(\boldsymbol{x},\boldsymbol{y}),\mathrm{JRATE}(\mathrm{XSEC}(\boldsymbol{x},\boldsymbol{y}),z)) \tag{4}$$

$$f_{\mathrm{mfg,assm}}(\boldsymbol{x},\boldsymbol{y},\boldsymbol{z}) = f_{\mathrm{mfg}}(\boldsymbol{x},\boldsymbol{y}) + f_{\mathrm{assm}}(\boldsymbol{z}) \tag{5}$$

$$f_{\mathrm{adj}}(\boldsymbol{x}) = -\sum_{p \in P(x)} \sum_{a \in \mathrm{KC}_p} \sum_{a \in \mathrm{CS}_p} (1 - |\mathbf{k}(a) \cdot \mathbf{n}(e)|) \tag{6}$$

where

$$f_{\mathrm{mfg}}(\mathbf{x},\mathbf{y}) = -\sum_{i=0}^{n} \{\mathrm{DIEC}(\mathrm{COMP}(i,\mathbf{x}),\mathbf{y}) + \mathrm{BNDC}(\mathrm{COMP}(i,\mathbf{x}))\} - \sum_{i=0}^{m-1} \mathrm{CASTC}(i,\boldsymbol{x}) \tag{7}$$

$$f_{\mathrm{assm}}(\mathbf{z}) = -\,C_w \sum_{i=0}^{m-1} \mathrm{WLDL}(i,z) \times \mathrm{WLDT}(i,z) \tag{8}$$

and n and m are the numbers of components and joints in a decomposed structure, respectively. DISP is the sum or maximum of the displacements at a predefined point(s) of the beam-torsional spring FE model of an assembled structure. The structural stiffness explained in Step 2 is calculated as the negative of this value. $\mathrm{XSEC}(\boldsymbol{x},\boldsymbol{y})$ is the cross-sectional properties of the components specified by $\boldsymbol{x}$ with the beam cross-sectional dimensions specified by y. JRATE is the torsional spring rates at each joint with cross-sectional properties XSEC and weld amount z. This function is

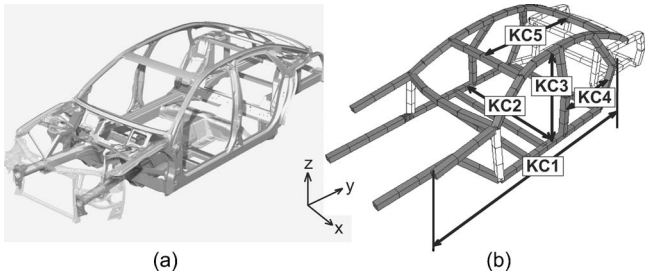

Fig. 12 (*a*) ASF for a passenger car and (*b*) simplified frame model used in the case study with 5 KCs (KC1∼KC5)

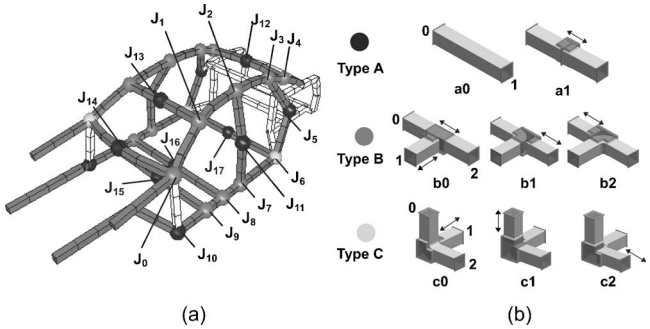

Fig. 13 (*a*) potential joint locations and (*b*) possible joint types (joint library) for each location type. Arrows in (*b*) indicate the adjustable directions.

computed using the ANNs that map the design variables to the torsional spring rates. $\mathrm{COMP}(i,\boldsymbol{x})$ is the i-th structural component specified by $\boldsymbol{x}$. DIEC and BNDC are the cost of extrusion die and bending operation of a component, respectively, and $\mathrm{CASTC}(i,\boldsymbol{x})$ is the casting cost at the ith joint specified by $\boldsymbol{x}$. The manufacturing cost explained in Step 2 is calculated as the negative of the sum of the DIEC and BNDC for all components plus the sum of the CASTC for all joint locations. C_w is the cost of welding operation per unit weld volume. $\mathrm{WLDL}(i,z)$ and $\mathrm{WLDT}(i,z)$ are the length and thickness of the welds at the ith joint as specified by z. The assembly cost explained in the Step 2 is calculated as the negative of the sum of the weld costs estimated from the weld volume, $\mathrm{WLDL}(i,\mathbf{z})\times\mathrm{WLDT}(i,\mathbf{z})$, for all joint locations. $P(\mathbf{x})$ is the set of all partitions p in the assembly defined by x. KC_p is the set of KCs of the p-th partitioning CS_p is the cut-set edges in the p-th partitioning a is the KC in the KC_p and e is a joint in CS_p. $\mathbf{k}(a)$ and $\mathbf{n}(e)$ are normal vector for a and e, respectively.

3.3.3 Formulation of Optimization Problem. Finally, the problem can be simply formulated as the following multiobjective optimization with no explicit constraints:

$$\begin{aligned}&\text{maximize:}\quad \{f_{\text{stiff}}(\boldsymbol{x},\boldsymbol{y},z),\ f_{\text{mfg,assm}}(\boldsymbol{x},\boldsymbol{y},z),\ f_{\text{adj}}(\boldsymbol{x})\}\\&\text{subject to:}\\&\qquad \boldsymbol{x}\in J_1\times J_2\times\cdots\times J_n\\&\qquad \boldsymbol{y}\in S^B\\&\qquad z\in W^n\end{aligned}\tag{9}$$

A modified nondominated sorting genetic algorithm-II (NSGA-II) [19] is used for the above problem due to the discrete nature of the design variables. Some enhancements to the conventional NSGA-II are made in the niching based on the distances in function domain and stochastic universal sampling, successfully applied in our previous works [19]. A chromosome $\boldsymbol{c}$ (an internal representation of design variables for genetic algorithms) is a simple list of the three design variables

$$\boldsymbol{c}=(\boldsymbol{x},\boldsymbol{y},z)\tag{10}$$

Since the information in $\boldsymbol{x}$, $\boldsymbol{y}$, and z are linked to the physical geometry of structure, the conventional one point or multiple point crossover for linear chromosomes are ineffective in preserving high-quality building blocks. For this type of problem, direct crossover has been successfully applied to improve the performance [20,21], whose details can be found in [5] along with the description of the modified NSGA-II.

4 Case Study

This section presents a case study on an aluminum space frame (ASF) of a passenger vehicle. This model was adopted from the case study model in [8] and additional design factors such as joint assembly directions are added to evaluate the dimensional adjustability (Fig. 13(*b*)). The actual vehicle design (Fig. 12(*a*)) is first simplified and five (5) KCs are assigned (Fig. 12(*b*)), where all frames are modeled as square tubes with identical external dimensions and with possibly different internal thicknesses. Assuming the left-right symmetry of the body, the design variables are assigned only to the left half of the body structure. A total of 30 possible joint locations are specified as in Fig. 13(*a*). These locations are classified as A, B, and C, each of which has feasible joint types in Fig. 13(*b*).

Based on the possible joint locations, 42 basic members are identified, from which structural topology graph G with 42 nodes and 66 edges is constructed. As in Fig. 14(*a*), variable $\boldsymbol{y}_i$ has two elements, y_{i0} and y_{i1}. The first element y_{i0} represents the upper/lower thickness of the beam when the beam is placed on the horizontal plane. In this case, the second element y_{i1} represents the side thickness of the beam. Similarly, when the beam is placed on a vertical plane, y_{i0} represents the front/back thickness of the beam while y_{i1} represents the side thickness of the beam. Figure 14(*b*) illustrates the definition of variable $\boldsymbol{z}_i$, where z_{i0} is the thickness of weld between cast and component 0 and $\boldsymbol{z}_{i1}$ is thethickness of weld between cast and component 1. While the nature of elements in $\boldsymbol{y}_i$ and $\boldsymbol{z}_i$ is a continuous value (length), those elements are discretized in ten steps between lower and upper boundary values.

The stiffness of the assembled structure is calculated considering the maximum displacement of floor frame under bending loads.

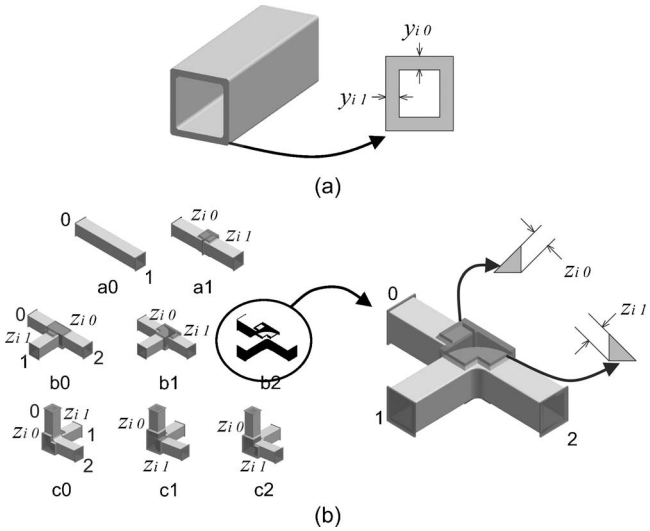

Fig. 14 (*a*) Beam cross-sectional design variable (beam thickness y_{i0} and y_{i1}) and (*b*) joint design variable (weld thickness, z_{i0} and z_{i1})

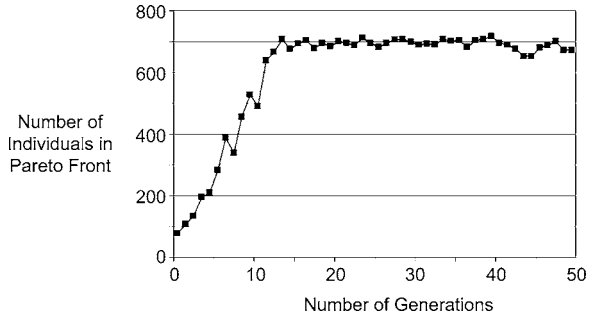

Fig. 15 Convergence history of GA run for the case study

As a training data for the artificial neural network (ANN), the detailed 3D FE models of seven joint types (a1, b0–*b*2, c0–c2) in Fig. 13(*b*) are analyzed. For each spring rate, a radial-basis neural network [22] is built with six input nodes (two ***y***'s for two joined frames and one **z** for the joint), 1250 hidden layer nodes, and 1 output node (joint rate) using MATLAB [23]. The networks are trained to reach a satisfactory convergence (rmserror $<10\%$).

For this model, entire design space can be estimated considering the design variables. When the symmetric design on left and right side of vehicle is considered, the joint configuration of total 18 possible joint locations (J_0–J_{17} in Fig. 13(*a*)) need to be decided. Based on the joint library in Fig. 13(*b*), about $2^{9*}3^9-10^7$ potential designs exist only in the joint configuration. By considering the beam cross section and welding design, total design space expands to an extremely large size ($\sim 10^{85}$). In this case study, therefore, a relatively large population number (1000) is used. The generation number was finalized after observing the convergence trends. Figure 15 shows the convergence histories of the GA run. This plot indicates the increase in the size of the Pareto set (number of Pareto optimal designs) as the number of generation increases. After 15 generations, the size of Pareto set was converged to about 700, which is 70% of the entire population. Based on this observation, total generation number was set as 50. Using a PC with hyperthreaded Pentium 4 3.07 GHz, one optimization run takes approximately two days. Most of the CPU time is used for the FE analysis of entire ASF model about 3 sec for one evaluation.

Table 1 Objective function values for Design R1–R2

	No. Comp.	f_{stiff}[mm]	$f_{\text{mfg,assm}}$[S]	f_{adj}
R1	12	**–0.059**	**–496.6**	–10,1000.0
R2	22	–0.703	–818.2	**–0.11**

Figure 16 shows the Pareto solutions at the terminal generation. Figure 16(*a*) shows 3D view of the Pareto set and 16(*b*)–16(*d*) illustrate 2D projection onto the two objectives. Two representative designs R1 and R2 are selected and their objective function values are listed in the Table 1.

Design R1 (Fig. 17(*a*)) shows good results both in stiffness and manufacturing/assembly cost. This structure has long one-piece rocker rails (C_1) with thick wall dimensions which seem to increase the stiffness of the structure under global bending loading. Also, this design minimizes the number of beam components (minimizing the extrusion dies) and joint casting components (minimizing number of casting sleeves) by not having joints at location type A (see Fig. 13), resulting in minimizing manufacturing and assembly costs. However, the small number of components limited the assembly directions to satisfy the five KCs, resulting in lower adjustability compared to the design R2.

Design R2 (Figs. 17(*b*) and 18) contains relatively thin-walled extrusion components in the rocker (C_1, C_2, and C_4), resulting the

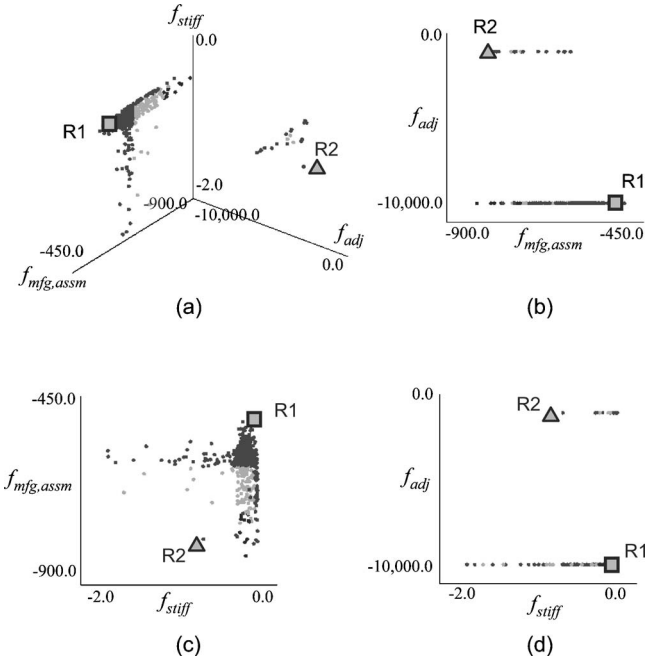

Fig. 16 Designs at the terminal condition (generation=50). Pareto solutions are colored as darker dots.

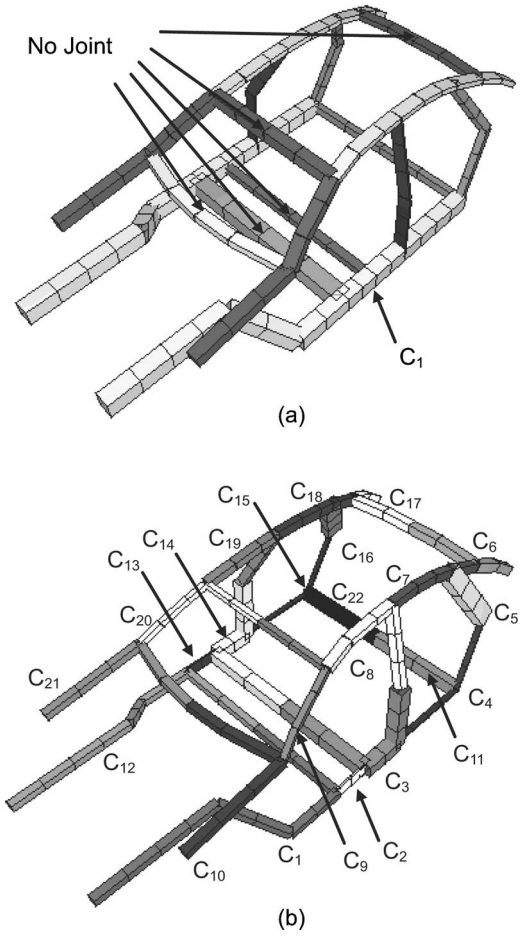

Fig. 17 Individual designs from Pareto set. (*a*) R1 with 12 components and (*b*) R2 with 22 components.

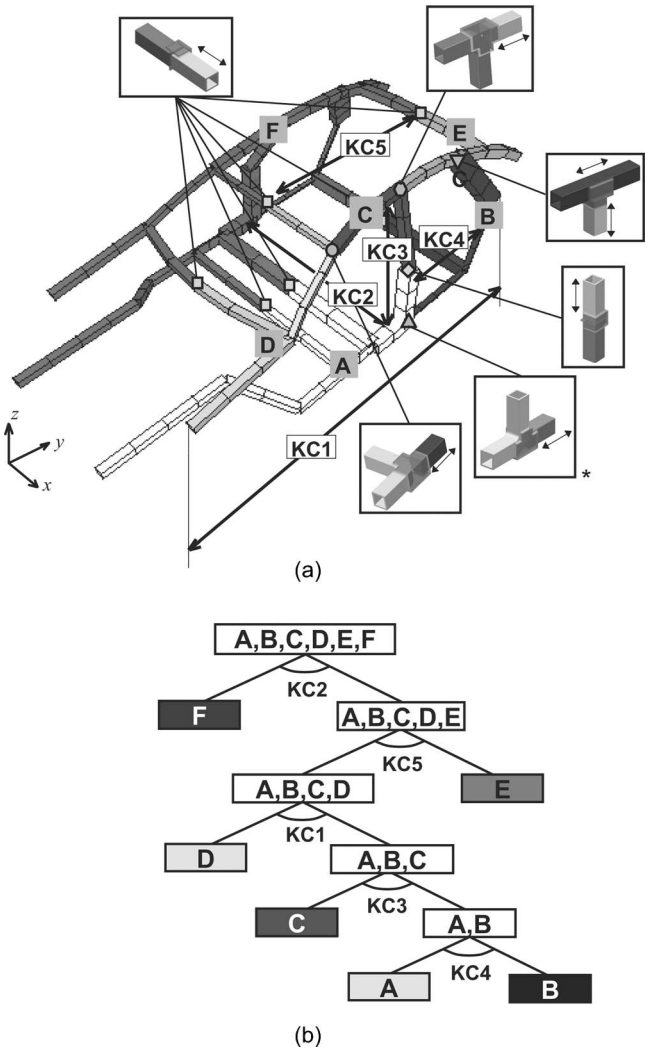

Fig. 18 Assembly partitioning of R2: (*a*) six subassemblies and (*b*) binary tree representation

large deflection of the floor. Also, this design contains a large number of components (22) that increased the manufacturing cost (by having more extrusion dies) and assembly cost (by having more number of joint locations requiring joining). However the large numbers of components accompanied by a large number of joints gave more freedom in the assembly procedures resulting in a very good adjustability that satisfies all five KCs. Figure 18 shows the assembly partitioning of R2, and Table 2 lists the components that comprise the subassemblies in Fig. 18(*a*). The assembly sequence that satisfying all five KCs is as follows:

1. A and B are assembled, satisfying KC4. Note that the assembly is done in the *y* direction and the joint between A and B (marked with * in Fig. 18(*a*)) allows the adjustment in the direction of KC4.
2. C and {A,B} are assembled parallel to KC3, satisfying KC3.
3. D and {A,B,C} are assembled in the *y* direction, satisfying KC1.
4. E and {A,B,C,D} are assembled, satisfying KC5.
5. F, a mirror image of {A,B,C,D,E}, is assembled in the same manner as {A,B,C,D,E}. F and {A,B,C,D,E} are assembled in the *x* direction, satisfying KC2.

Table 2 Subassemblies for Design R2

Subassembly	R2 Components in Fig. 18
A	$C_1 \sim C_3$
B	$C_4 \sim C_5, C_{11}$
C	C_8
D	$C_9 \sim C_{10}$
E	$C_5 \sim C_7$
F	$C_{12} \sim C_{21}$

5 Summary

This paper described an extension of our previous work on decomposition-based assembly synthesis [3–8], which integrates the consideration on structural stiffness and manufacturing and assembly costs [5,8], and dimensional integrity [4,6,7], under an unified framework of multiobjective optimization using joint libraries. The optimization problem is posed as a simultaneous determination of the location and feasible types of joints in a structure selected from the predefined joint libraries, combined with the size optimization for the cross sections of the joined structural frames. The structural stiffness is evaluated by finite element analyses of a beam-spring model modeling the joints and joined frames. Manufacturing and assembly costs are estimated based on the geometries of the components and joints. Dissimilar to the enumerative approach in [6,7], dimensional integrity of a candidate assembly is evaluated as the adjustability of the given critical dimensions, using an internal optimization routine that finds the optimal subassembly partitioning of an assembly for in-process adjustability [4]. The optimization problem is solved by a multiobjective genetic algorithm. The case study on an ASF of the midsize passenger vehicle clearly demonstrates the effectiveness of the method in synthesizing multiple high-quality designs with different tradeoffs among the given objectives, each of which can be further examined by the human designer during the detailed design phase.

Acknowledgment

The authors acknowledge funding provided by Toyota Motor Corporation and National Science Foundation under CAREER Award (DMI-9984606) for this research. We thank Mr. Karim Hamza at Discrete Design Optimization Laboratory at the University of Michigan for providing his FEM code. Any opinions, findings, and conclusions or recommendations expressed in this material are those of the authors and do not necessarily reflect the views of the National Science Foundation.

References

[1] Lee, D. J., and Thornton, A. C., 1996, "The Identification and Use of Key Characteristics in the Product Development Process," *1996 ASME Design Engineering Technical Conference*, Irvine, California, Paper No. 96-DETC/DTM-1506, American Society of Mechanical Engineers, New York, NY.
[2] Whitney, D. E., Mantripragada, R., Adams, J. D., and Rhee, S. J., 1999, "Designing Assemblies," Res. Eng. Des., **11**, pp. 229–253.
[3] Yetis, A., and Saitou, K., 2002, "Decomposition-Based Assembly Synthesis Based on Structural Considerations," J. Math. Biol., **124**, pp. 593–601.
[4] Lee, B., and Saitou, K., 2003, "Assembly Synthesis with Subassembly Partitioning for Optimal In-Process Dimensional Adjustability," Proceedings of the 2003 ASME DETC, Chicago, IL, DETC2003/DAC-48729, American Society of Mechanical Engineers, New York, NY
[5] Lyu, N., and Saitou, K., 2005, "Decomposition-Based Assembly Synthesis of a Three Dimensional Body-In-White Model for Structural Stiffness," J. Math. Biol., **127**(1), pp. 34–48.
[6] Lee, B., and Saitou, K., 2003, "Decomposition-based Assembly Synthesis for In-Process Dimensional Adjustability," J. Math. Biol., **125**(3), pp. 464–473.
[7] Lee, B., and Saitou, K., 2006, "Three-Dimensional Assembly Synthesis for Robust Dimensional Integrity Based on Screw Theory," J. Math. Biol., January, **128**(1), pp. 57–65.
[8] Lyu, N., and Saitou, K., 2006, "Decomposition-Based Assembly Synthesis of Space Frame Structures using Joint Library," J. Math. Biol., January, **128**(1), pp. 243–251.

[9] Boothroyd, G., and Dewhurst, P., 1983, *Design for Assembly Handbook*, University of Massachusetts, Amherst, MA.
[10] Chang, D., 1974, "Effects of Flexible Connections on Body Structural Response," SAE Q. Trans., **83**, pp. 233–244.
[11] Lee, K., and Nikolaidis, E., 1992, "A Two-Dimensional Model for Joints in Vehicle Structures," Comput. Struct., **45**(4), pp. 775–784.
[12] Kim, Y. Y., and Kim, H., J., 2002, "New Accurate Efficient Modeling Techniques for the Vibration Analysis of T-Joint Thin-Walled Box Structures," Int. J. Solids Struct., **39**, pp. 2893–2909.
[13] Long, L., 1998, Design-Oriented Translators for Automotive Joints, Ph.D. thesis, Virginia Polytechnic Institute.
[14] Overhagh, W. H., 1995, "Use of Aluminum in Automotive Space Frame," SAE Technical Paper, 950721, International Congress and Exposition, Detroit, MI, Society of Automotive Engineers, Detroit, MI.
[15] von Zengen, K.-H., and Leitermann, W. 1998, "Space Frame - Quo Vadis?" SAE Technical Paper, 982401, International Body Engineering Conference and Exposition, Detroit, MI, Society of Automotive Engineers, Detroit, MI.
[16] Audi, A. G., http://www.audi.com
[17] Ahmetoglu, M. A., 2000, "Manufacturing of Structural Automotive Components from Extruded Aluminum Profiles," SAE Technical Paper 2000-01-2712, International Body Engineering Conference, Detroit, MI, Society of Automotive Engineers, Detroit, MI.
[18] Chung, T., Lee, Y., and Kim, C., 1995, "Joint Design Approach for Aluminum Space Frame," SAE Technical Paper 950577, International Congress and Exposition, Detroit, MI, Society of Automotive Engineers, Detroit, MI.
[19] Homem de Mello, L. S., and Sanderson, A. C., 1990, "AND/OR Graph Representation of Assembly Plans," IEEE Trans. Rob. Autom., **6**(2), pp. 188–199.
[20] Deb., K., Agrawal, S., Pratab, A., and Meyarivan, T., 2000, "A Fast Elitist Non-Dominated Sorting Genetic Algorithm for Multi-Objective Optimization: NSGA-II," KanGAL Report No. 200001, Indian Institute of Technology, Kanpur, India.
[21] Lyu, N., and Saitou, K., 2005, "Topology Optimization of Multi-Component Beam Structures via Decomposition-Based Assembly Synthesis," J. Math. Biol., **127**(2), pp. 170–183.
[22] Pereira, F., Machado, P., Costa, E., and Cardoso, A., 1999, "Graph Based Crossover—A Case Study with the Busy Beaver Problem," Proceedings of the 1999 Genetic and Evolutionary Computation Conference, Orlando, FL.
[23] Chen, S., Cowan, C., and Grant, P. M., 1991, "Orthogonal least squares learning algorithm for radial basis function networks," IEEE Trans. Neural Netw., **2**(2), pp. 302–309.
[24] The MathWorks, Matlab, The language of Technical Computing, 6.0.0.88, Release 12, http://mathworks.com